Computers and Structures 147 (2015) 138–146

Contents lists available at ScienceDirect

Computers and Structures

journal homepage: www.elsevier.com/locate/compstruc

T-spline based XIGA for fracture analysis of orthotropic media

S.Sh. Ghorashi [a,*], N. Valizadeh [b], S. Mohammadi [c], T. Rabczuk [b,*]

[a] Research Training Group 1462, Bauhaus-Universität Weimar, Weimar, Germany
[b] Institute of Structural Mechanics, Bauhaus-Universität Weimar, Weimar, Germany
[c] School of Civil Engineering, University of Tehran, Tehran, Iran

ARTICLE INFO

Article history:
Accepted 29 September 2014
Available online 22 October 2014

Keywords:
Orthotropic media
Crack
Extended isogeometric analysis (XIGA)
Orthotropic enrichment functions
T-spline basis functions
Local refinement

ABSTRACT

Fracture analysis of orthotropic cracked media is investigated by applying the recently developed extended isogeometric analysis (XIGA) (Ghorashi et al., 2012) using the T-spline basis functions. The signed distance function and orthotropic crack tip enrichment functions are adopted for extrinsically enriching the conventional isogeometric analysis approximation for representation of strong discontinuity and reproducing the stress singular field around a crack tip, respectively. Moreover, by applying the T-spline basis functions, XIGA is further developed to make the local refinement feasible. For increasing the integration accuracy, the 'sub-triangle' and 'almost polar' techniques are adopted for the cut and crack tip elements, respectively. The interaction integral technique developed by Kim and Paulino (2003) is applied for computing the mixed mode stress intensity factors (SIFs). Finally, the proposed approach is applied for analysis of some cracked orthotropic problems and the mixed mode SIFs are compared with those of other methods available in the literature.

1. Introduction

Orthotropic materials such as composites have been increasingly applied in many engineering applications e.g. aerospace, automobile and marine structures because of their high strength and stiffness to weight ratios. Considering their strength, they are applied in thin shell forms with the possibility of crack initiation and propagation. As a result, fracture analysis of such media has been the center of attention for many researchers in the past few decades.

Analytical solution of stress and displacement fields for an orthotropic plate with a crack has already been obtained by Sih et al. [3]. Some other analytical investigations on fracture behavior of composites can be found in [4–10]. As the analytical methods are not feasible in resolving practical engineering problems, numerical methods are better alternatives.

The remeshing requirement and the existence of singular fields around crack tips in simulation of crack propagation problems led to the development of several computational approaches such as meshfree methods [11–21] and the extended finite element method (XFEM) [22–24]. Problems involving with moving discontinuities such as crack propagation can be analyzed by these methods without the requirement of remeshing or rearranging of the nodal points. Some applications of these methods can be found in [25–31]. In XFEM, a priori knowledge of the solution is locally added to the approximation space. This enrichment allows for accurate capture of particular features such as discontinuities and singularities which are present in the solution.

In order to analyze the problem of cracked orthotropic bodies different approaches have been applied such as the hybrid-displacement finite element method [32], the boundary element method (BEM) [33], finite elements and the modified crack closure method [34]. Asadpoure et al. [35–37] succeeded in developing three sets of orthotropic enrichment functions for different types of composites using the analytical solutions and implemented them within an XFEM framework. The general form of orthotropic enrichment functions [37] have also been adopted in the enriched element free Galerkin (EFG) method [38]. Further developments have been reported for dynamics and moving cracks in orthotropic media [39,40] and delamination analysis of composites [41].

Although cracked orthotropic media have been studied by several different methods, the new developments in the promising computational approach of the extended isogeometric analysis (XIGA) [42,1] have attracted new investigations to further apply it for such problems.

* Corresponding authors at: Civil Engineering Department, Bauhaus-Universität Weimar, Weimar, Germany.
E-mail addresses: shahram.ghorashi@uni-weimar.de (S.Sh. Ghorashi), navid.valizadeh@uni-weimar.de (N. Valizadeh), smoham@ut.ac.ir (S. Mohammadi), timon.rabczuk@uni-weimar.de (T. Rabczuk).

http://dx.doi.org/10.1016/j.compstruc.2014.09.017
0045-7949/

XIGA takes the advantages of its two origins: the extended finite element method (XFEM) and the isogeometric analysis (IGA) [43]. IGA integrates the computer aided design (CAD) into the finite element method (FEM) using the concept of isoparametric elements, in which the same shape functions are used to represent the geometry and to approximate the solution. Its superiorities over conventional FEM are: capability of exact representation of complex geometries regardless of the mesh coarseness, simplification of the refinement process and improvement of the solution accuracy. A large variety of problems [44–46] have already been solved by IGA. XIGA has been successfully applied for simulation of stationary and propagating cracks in 2D linear-elastic isotropic media [1]. Ghorashi et al. have further enhanced XIGA for analysis of curved cracks [47]. In addition, more results have been reported on crack detection using the XIGA [48]. Recently, the XIGA has been also applied for analysis of material interface problems and the techniques for achieving optimal convergence rates have been addressed [49].

The current XIGA method adopts the conventional NURBS basis function which has a considerable drawback. The local refinement cannot be defined within it because it is based on a tensor-product structure which requires the control points to lie topologically in a rectangular grid. In other words, when a control point needs to be added, several superfluous control points should be defined. One solution is to use multiple patches, which has also some limitations. The compatibility of adjacent NURBS patches on their interfaces has to be maintained. Generally, the refinement extends from one patch to another unless the compatibility between patches are enforced in a different way. One can weakly enforce it by the variational formulation applying the discontinuous Galerkin formulation. Another alternative is to enforce C^0 continuity on the interfaces between patches [50] by utilizing constraint equations for the control points and variables. IGA formulations based on triangular splines [51] might be an interesting alternative as they simplify the mesh generation and adaptive refinement procedure.

A more enchanting solution for the aforementioned problem is to use the so-called T-splines [52–54], which are a generalization of NURBS, by allowing a row of control points to terminate before reaching the patch boundary. This feature enables the truly local refinement without extending the entire row of control points. Furthermore, by using the T-splines several NURBS patches that have different knot vectors can be efficiently merged into a single gap-free model of C^0 or higher order continuity [53]. Recently, a subset class of T-splines called "analysis-suitable T-splines", which are linearly independent, has been introduced in the IGA framework [55] and a highly localized refinement algorithm which meets the demands of both design and analysis has been presented [56].

Another alternative to T-splines are PHT-splines or RHT-splines that are based on hierarchical T-meshes [57]. Continuum and structural element formulations based on PHT- and RHT-splines have been developed in [58–60], respectively.

In this contribution, XIGA is further extended and the T-spline basis functions which belong to the analysis-suitable T-splines are adopted to make the local refinement for feasible adaptive procedure. Furthermore, based upon the work of Ghorashi et al. [61], the orthotropic enrichment functions [37] are adopted to investigate cracked orthotropic bodies.

In Section 2, important formulations of orthotropic materials are introduced. Basis functions including NURBS and T-splines are then described in Section 3. Thereafter, the proposed XIGA method including orthotropic enrichment functions is presented in Section 4. The results obtained from the present orthotropic XIGA and those available in the literature are compared in Section 5 to demonstrate the accuracy and efficiency of the proposed approach. This is achieved by implementing the interaction integral technique, developed by Kim and Paulino [2], for computation of mixed mode stress intensity factors. This section is followed by some concluding remarks in Section 6.

2. Fracture mechanics in orthotropic media

The stress–strain law in an arbitrary linear elastic material can be written as

$$\boldsymbol{\varepsilon} = \boldsymbol{c}\boldsymbol{\sigma} \tag{1}$$

where $\boldsymbol{\varepsilon}$ and $\boldsymbol{\sigma}$ are the strain and stress vectors, respectively, and $\mathbf{c}$ is the compliance matrix,

$$\mathbf{c}^{3D} = \begin{bmatrix} \frac{1}{E_1} & -\frac{v_{21}}{E_2} & -\frac{v_{31}}{E_3} & 0 & 0 & 0 \\ -\frac{v_{12}}{E_1} & \frac{1}{E_2} & -\frac{v_{32}}{E_3} & 0 & 0 & 0 \\ -\frac{v_{13}}{E_1} & -\frac{v_{23}}{E_2} & \frac{1}{E_3} & 0 & 0 & 0 \\ 0 & 0 & 0 & \frac{1}{G_{23}} & 0 & 0 \\ 0 & 0 & 0 & 0 & \frac{1}{G_{13}} & 0 \\ 0 & 0 & 0 & 0 & 0 & \frac{1}{G_{12}} \end{bmatrix} \tag{2}$$

where E, v and G are Young's modulus, Poisson's ratio and shear modulus, respectively. For a plane stress case, the compliance matrix is reduced to the following form:

$$\mathbf{c}^{2D} = \begin{bmatrix} \frac{1}{E_1} & -\frac{v_{21}}{E_2} & 0 & 0 & 0 & 0 \\ -\frac{v_{21}}{E_2} & \frac{1}{E_2} & 0 & 0 & 0 & 0 \\ 0 & 0 & 0 & 0 & 0 & 0 \\ 0 & 0 & 0 & 0 & 0 & 0 \\ 0 & 0 & 0 & 0 & 0 & 0 \\ 0 & 0 & 0 & 0 & 0 & \frac{1}{G_{12}} \end{bmatrix} \tag{3}$$

and for a plane strain state,

$$c_{ij}^{2D} = c_{ij}^{3D} - \frac{c_{i3}^{3D} c_{j3}^{3D}}{c_{33}^{3D}} \quad \text{for } i,j = 1,2,6 \tag{4}$$

Now assume an anisotropic body is subjected to arbitrary forces with general boundary conditions and a crack. The global Cartesian coordinate (X_1, X_2), the local Cartesian coordinate (x, y) and the local polar coordinate (r, θ), defined on the crack tip, are illustrated in Fig. 1. A fourth-order partial differential equation with the following characteristic equation can be obtained from the equilibrium and compatibility conditions [5],

$$c_{11}s^4 - 2c_{16}s^3 + (2c_{12} + c_{66})s^2 - 2c_{26}s + c_{22}0 = 0 \tag{5}$$

where c_{ij} $(i,j = 1,2,6)$ are the components of $\mathbf{c}^{2D}$. According to [5], the roots of Eq. (5) are always complex or purely imaginary $(s_k = s_{kx} + is_{ky}, \quad k = 1,2)$ and occur in conjugate pairs as $s_1, \bar{s}_1$

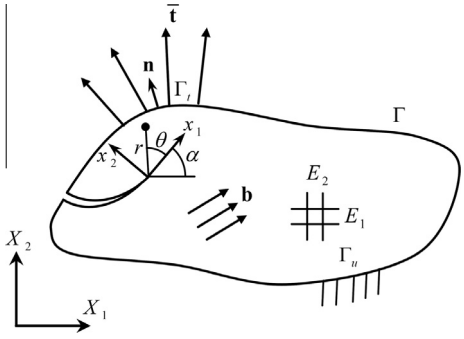

Fig. 1. An arbitrary orthotropic cracked body subjected to body force **b** and traction $\bar{\mathbf{t}}$.

and s_2, $\bar{s_2}$. The two-dimensional displacement and stress fields in the vicinity of the crack-tip can then be derived as [3]

– Mode I

$$\begin{aligned} u^I &= K_I\sqrt{\frac{2r}{\pi}}\mathrm{Re}\left[\frac{1}{s_1-s_2}\left(s_1p_2\sqrt{\cos\theta+s_2\sin\theta}-s_2p_1\sqrt{\cos\theta+s_1\sin\theta}\right)\right]\\ v^I &= K_I\sqrt{\frac{2r}{\pi}}\mathrm{Re}\left[\frac{1}{s_1-s_2}\left(s_1q_2\sqrt{\cos\theta+s_2\sin\theta}-s_2q_1\sqrt{\cos\theta+s_1\sin\theta}\right)\right]\\ w^I &= 0 \end{aligned} \tag{6}$$

$$\begin{aligned} \sigma^I_{xx} &= \frac{K_I}{\sqrt{2\pi r}}\mathrm{Re}\left[\frac{s_1s_2}{s_1-s_2}\left(\frac{s_2}{\sqrt{\cos\theta+s_2\sin\theta}}-\frac{s_1}{\sqrt{\cos\theta+s_1\sin\theta}}\right)\right]\\ \sigma^I_{yy} &= \frac{K_I}{\sqrt{2\pi r}}\mathrm{Re}\left[\frac{1}{s_1-s_2}\left(\frac{s_1}{\sqrt{\cos\theta+s_2\sin\theta}}-\frac{s_2}{\sqrt{\cos\theta+s_1\sin\theta}}\right)\right]\\ \sigma^I_{xy} &= \frac{K_I}{\sqrt{2\pi r}}\mathrm{Re}\left[\frac{s_1s_2}{s_1-s_2}\left(\frac{1}{\sqrt{\cos\theta+s_1\sin\theta}}-\frac{1}{\sqrt{\cos\theta+s_2\sin\theta}}\right)\right] \end{aligned} \tag{7}$$

– Mode II

$$\begin{aligned} u^{II} &= K_{II}\sqrt{\frac{2r}{\pi}}\mathrm{Re}\left[\frac{1}{s_1-s_2}\left(p_2\sqrt{\cos\theta+s_2\sin\theta}-p_1\sqrt{\cos\theta+s_1\sin\theta}\right)\right]\\ v^{II} &= K_{II}\sqrt{\frac{2r}{\pi}}\mathrm{Re}\left[\frac{1}{s_1-s_2}\left(q_2\sqrt{\cos\theta+s_2\sin\theta}-q_1\sqrt{\cos\theta+s_1\sin\theta}\right)\right]\\ w^{II} &= 0 \end{aligned} \tag{8}$$

$$\begin{aligned} \sigma^{II}_{xx} &= \frac{K_{II}}{\sqrt{2\pi r}}\mathrm{Re}\left[\frac{1}{s_1-s_2}\left(\frac{s_2^2}{\sqrt{\cos\theta+s_2\sin\theta}}-\frac{s_1^2}{\sqrt{\cos\theta+s_1\sin\theta}}\right)\right]\\ \sigma^{II}_{yy} &= \frac{K_{II}}{\sqrt{2\pi r}}\mathrm{Re}\left[\frac{1}{s_1-s_2}\left(\frac{1}{\sqrt{\cos\theta+s_2\sin\theta}}-\frac{1}{\sqrt{\cos\theta+s_1\sin\theta}}\right)\right]\\ \sigma^{II}_{xy} &= \frac{K_{II}}{\sqrt{2\pi r}}\mathrm{Re}\left[\frac{1}{s_1-s_2}\left(\frac{s_1}{\sqrt{\cos\theta+s_1\sin\theta}}-\frac{s_2}{\sqrt{\cos\theta+s_2\sin\theta}}\right)\right] \end{aligned} \tag{9}$$

where Re denotes the real part of the statement and K_1 and K_{II} are stress intensity factors for modes I and II, respectively. p_i and q_i can be defined by

$$p_i = c_{11}s_i^2 + c_{12} - c_{16}s_i, \quad (i=1,2) \tag{10}$$

$$q_i = c_{12}s_i + \frac{c_{22}}{s_i} - c_{26}, \quad (i=1,2) \tag{11}$$

3. Basis functions

3.1. NURBS

Non-uniform rational B-splines (NURBS) are a generalization of piecewise polynomial B-spline curves. The B-spline basis functions are defined in a parametric space on a knot vector Ξ. A knot vector in one dimension is a non-decreasing sequence of real numbers:

$$\Xi = \{\xi_1, \xi_2, \ldots, \xi_{n+p+1}\} \tag{12}$$

where ξ_i is the ith knot, i is the knot index, $i = 1,2,\ldots,n+p+1$, p is the degree of the B-spline, and n is the number of basis functions. The half open interval $[\xi_i, \xi_{i+1})$ is called the ith knot span and it can have zero length since knots may be repeated more than once, and the interval $[\xi_1, \xi_{n+p+1}]$ is called a patch. In the isogeometric analysis, always open knot vectors are employed. A knot vector is called open if it contains $p+1$ repeated knots at the two ends.

With a certain knot span, the B-spline basis functions are defined recursively as,

$$N_i^0(\xi) = \begin{cases} 1 & \text{if } \xi_i \leqslant \xi < \xi_{i+1} \\ 0 & \text{otherwise} \end{cases} \tag{13}$$

and

$$\begin{aligned} N_i^p(\xi) &= \frac{\xi-\xi_i}{\xi_{i+p}-\xi_i}N_i^{p-1}(\xi) + \frac{\xi_{i+p+1}-\xi}{\xi_{i+p+1}-\xi_{i+1}}N_{i+1}^{p-1}(\xi)\ p\\ &= 1,2,3,\ldots \end{aligned} \tag{14}$$

where $i = 1,2,\ldots,n$.

A B-spline curve of degree p is defined by:

$$\mathbf{C}(\xi) = \sum_{i=1}^{n} N_i^p(\xi)\mathbf{P}_i \tag{15}$$

where $N_i^p(\xi)$ is the ith B-spline basis function of degree p and $\{\mathbf{P}_i\}$ are the control points, given in d-dimensional space $\mathbf{R}^d$.

The non-uniform rational B-spline (NURBS) curve of degree p is defined as:

$$\mathbf{C}(\xi) = \sum_{i=1}^{n} R_i^p(\xi)\mathbf{P}_i \tag{16}$$

$$R_i^p(\xi) = \frac{N_i^p(\xi)w_i}{\sum_{j=1}^{n} N_j^p(\xi)w_j} \tag{17}$$

where $\{R_i^p\}$ are the NURBS basis functions and w_i is the ith weight that must be non-negative. In the two dimensional parametric space $[0,1]^2$, NURBS surfaces are constructed by tensor product through knot vectors $\Xi^1 = \{\xi_1^1, \xi_2^1, \ldots, \xi_{n+p+1}^1\}$ and $\Xi^2 = \{\xi_1^2, \xi_2^2, \ldots, \xi_{m+q+1}^2\}$. It yields to:

$$R_{i,j}^{p,q}(\xi^1,\xi^2) = \frac{N_i^p(\xi^1)M_j^q(\xi^2)w_{i,j}}{\sum_{k=1}^{n}\sum_{l=1}^{m} N_k^p(\xi^1)M_l^q(\xi^2)w_{k,l}} \tag{18}$$

For more details on NURBS, refer to [62].

3.2. T-splines

T-splines functions are a generalization of NURBS which allow termination of a row of control points before reaching the patch boundary [52–54]. T-spline basis functions are defined in a trimmed index space entitled "T-mesh". Trimmed index space is similar to the index space representing the NURBS where the first and last n_o knots of the global knot vectors are neglected. n_o equals to $(p+1)/2$ and $p/2$ for odd and even polynomial degrees, respectively. T-mesh is a trimmed index space where T-junctions, which are vertices connecting three edges, are allowed. An example of T-mesh is illustrated in Fig. 2. It is noted that each line in the mesh corresponds to a knot value of the trimmed global knot vector. Then, anchors are defined on the T-mesh to identify the location of each basis function. In each parametric direction, anchors are located on the lines if the corresponding polynomial degree is odd. Otherwise, their locations are assumed in the middle of the lines. Regardless of the degree, an anchor location is at the center of the support of a function in the index space.

For definition of T-splines, local knot vectors are defined instead of using the global knot vectors since each basis function has the compact support of $(p+1)\times(q+1)$ knots. As illustrated in Fig. 3, local knot vectors in each direction are defined by horizontally or vertically marching from the anchors backward and forward [53]. Afterwards, each basis function $T_\alpha^{p,q}(\xi^1,\xi^2)$ can be defined using Eqs. (13), (14) and (18)its corresponding local knot vectors Ξ_α^1 and Ξ_α^2.

In order to refine the mesh, the knot insertion process is performed. It consists of adding new knots to the present (T-) mesh

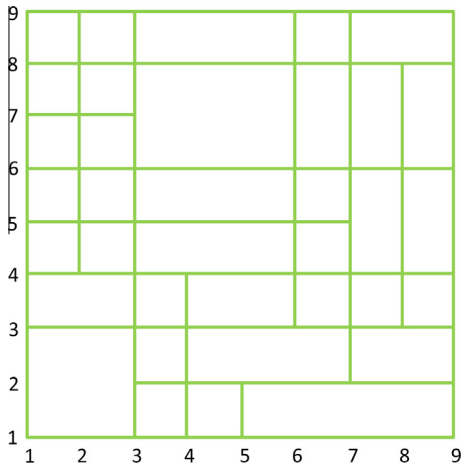

Fig. 2. A sample of T-mesh.

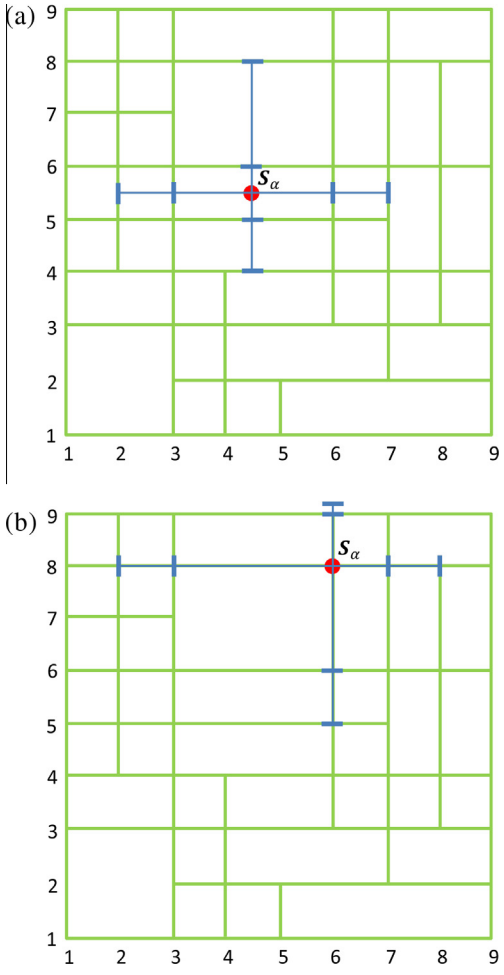

Fig. 3. Schematic view of defining local knot vectors for the anchor $\mathbf{S}_\alpha$: (a) quadratic polynomial degrees: $\Xi_\alpha^1 = \{\xi_2^1, \xi_3^1, \xi_6^1, \xi_7^1\}$ and $\Xi_\alpha^2 = \{\xi_4^2, \xi_5^2, \xi_6^2, \xi_8^2\}$; (b) cubic polynomial degrees: $\Xi_\alpha^1 = \{\xi_2^1, \xi_3^1, \xi_6^1, \xi_7^1, \xi_8^1\}$ and $\Xi_\alpha^2 = \{\xi_5^2, \xi_6^2, \xi_8^2, \xi_9^2, \xi_9^2\}$.

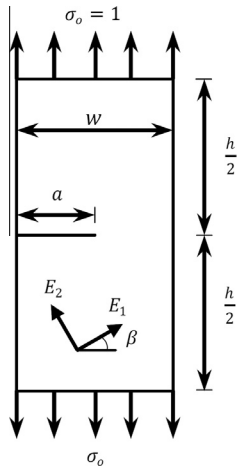

Fig. 4. Geometry and loading of the orthotropic rectangular plate with an edge crack.

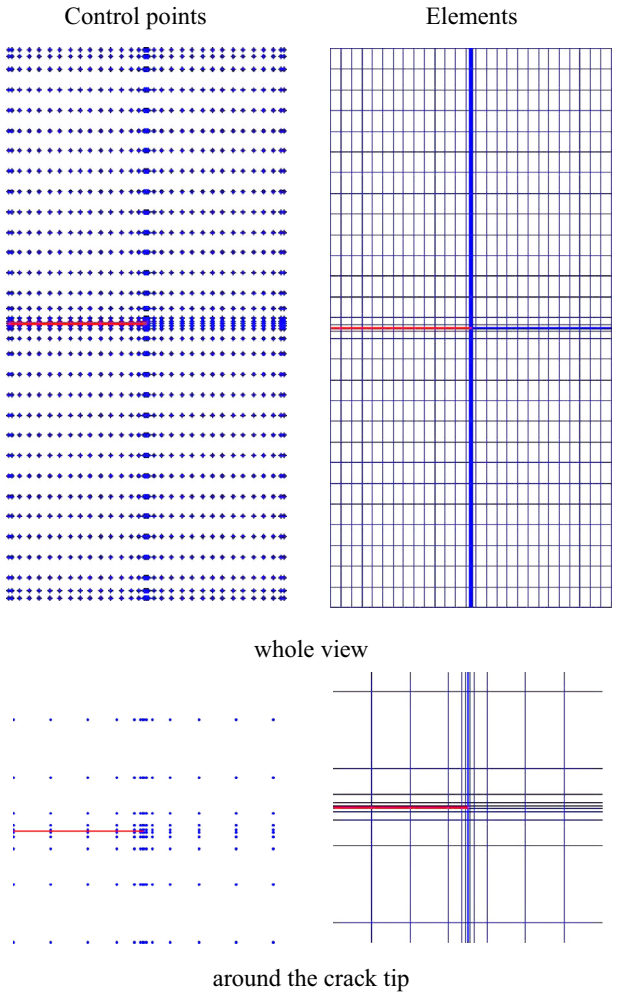

Fig. 5. Discretization of the globally refined model of the rectangular orthotropic plate.

and correspondingly, modifying and adding some control points. For more information about T-spline and local refinement, readers are referred to [52–54].

The T-splines applied in this paper are analysis-suitable T-splines [55]. Analysis-suitable T-splines are a set of T-splines whose T-mesh satisfies some topological conditions. It can contain T-junctions but L-junctions, I-junctions and isolated nodes are not allowed and their extension graphs should be empty [55,56]. Satisfying the above conditions, assures linear independence of T-spline's blending functions [55]. Readers are referred to [55,56] for more details.

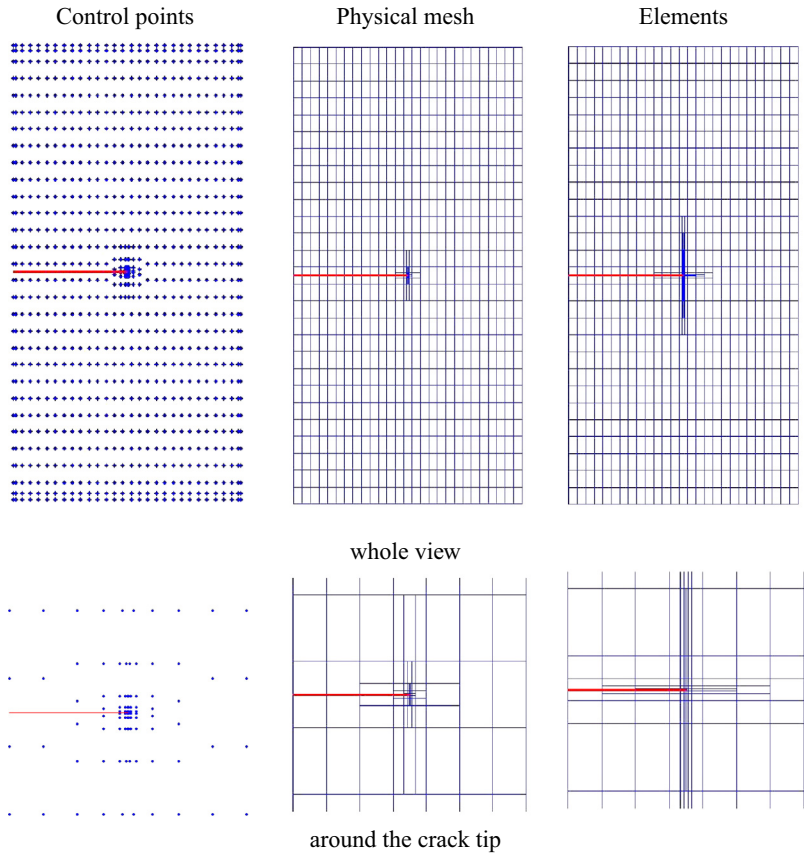

Fig. 6. Discretization of the locally refined model of the rectangular orthotropic plate.

4. Extended isogeometric analysis

The extended isogeometric analysis (XIGA) [42,1] is a newly developed computational approach which uses the superior concepts of the extended finite element method (XFEM) [22,23] within the isogeometric analysis method [43]. As a result, a crack can be modeled independently of the mesh and can propagate without the necessity of remeshing since the computational domain discretization is defined independently of the crack location.

While applying the NURBS basis functions has some limitations in the local refinement, adopting the T-spline basis functions in the XIGA allows for efficient introductions of local refinement and avoiding refining the unnecessary parts [63].

The geometry description is then defined as,

$$\mathbf{X}(\xi^1,\xi^2)=\sum_{i=1}^{n_{en}} T_i^{p,q}(\xi^1,\xi^2)\mathbf{P}_i \tag{19}$$

where n_{en} is the number of nonzero basis functions for a given knot span and $\{T_i^{p,q}(\xi^1,\xi^2)\}$are the T-Spline basis functions of degrees p and q in ξ^1 and ξ^2 directions, respectively, at the point (ξ^1,ξ^2) in the parametric space $[0,1]\times[0,1]$.

The solution field approximation is extrinsically enriched by the Heaviside and branch functions for representing the crack face and the singular stress field around the crack tip, respectively,

$$\mathbf{u}^h(\xi^1,\xi^2)=\sum_{i=1}^{n_{en}} T_i^{p,q}(\xi^1,\xi^2)\mathbf{u}_i+\sum_{j=1}^{n_H} T_j^{p,q}(\xi^1,\xi^2)H\mathbf{a}_j + \sum_{k=1}^{n_Q} T_k^{p,q}(\xi^1,\xi^2)\sum_{\alpha=1}^{4} Q_\alpha \mathbf{b}_k^\alpha \tag{20}$$

The first term in the right hand side is the standard T-spline based isogeometric analysis approximation. $\{\mathbf{a}_j\}$are the vectors of additional degrees of freedom which are related to the modeling of crack faces, $\{\mathbf{b}_k^\alpha\}$are the vectors of additional degrees of freedom for modeling the crack tip, n_Q is the number of n_{en} basis functions which are selected as branch enriched basis functions. They can be selected using the topological enrichment strategy or the geometrical enrichment approach. In the topological enrichment scheme, the basis functions which contain the crack tip in their influence domains are selected as the branch enriched basis functions while in the geometrical enrichment method, branch enriched basis functions consist of the basis functions chosen from the previous strategy and the ones which are selected according to considering a constant domain around the crack tip. In this contribution, the topological enrichment method is adopted. n_H is the number of n_{en} basis functions that have crack face in their support domains and have not been selected as branch enriched basis functions. H is the generalized Heaviside function [23],

$$H(\mathbf{X})=\begin{cases}+1 & \text{if } (\mathbf{X}-\mathbf{X}^*)\cdot\mathbf{e}_n>0\\ -1 & \text{otherwise}\end{cases} \tag{21}$$

where $\mathbf{e}_n$ is the unit normal vector of crack alignment in point $\mathbf{X}^*$on the crack surface which is the nearest point to $\mathbf{X}(\xi^1,\xi^2)$.

In Eq. (20), $Q_\alpha\{\alpha=1,2,3,4\}$are the crack tip enrichment functions whose roles are to reproduce the singular field around the crack tips. In this paper, the following orthotropic crack tip enrichment functions, developed by Asadpoure and Mohammadi [37], which were defined based on the analytical solution (Eqs. (6)–(9)), are adopted,

$$\{Q_\alpha\}_{\alpha=1}^{4} = \left\{ \sqrt{r}\cos\frac{\theta_1}{2}\sqrt{g_1(\theta)}, \sqrt{r}\cos\frac{\theta_2}{2}\sqrt{g_2(\theta)}, \sqrt{r}\sin\frac{\theta_1}{2}\sqrt{g_1(\theta)}, \sqrt{r}\sin\frac{\theta_2}{2}\sqrt{g_2(\theta)} \right\} \tag{22}$$

with

$$\theta_i = \arctan\left[\frac{s_{iy}\sin\theta}{\cos\theta + s_{ix}\sin\theta}\right], \quad (i = 1,2) \tag{23}$$

$$g_i(\theta) = \sqrt{(\cos\theta + s_{ix}\sin\theta)^2 + (s_{iy}\sin\theta)^2}, \quad (i = 1,2) \tag{24}$$

where s_{ix} and s_{iy} are real and imaginary parts of s_i computed by Eq. (5). It is noted that the third and fourth functions in the right-hand side of the Eq. (22) are discontinuous across the crack faces while the first and second ones remain continuous.

5. Numerical example

In order to evaluate the efficiency and validity of the proposed approach, two numerical examples are considered. The first one is a rectangular plate with an edge crack subjected to distributed tension loads and the other one is a circular shape containing an inclined central crack. Cubic and quadratic basis functions are adopted for the first and second examples, respectively. The effects of change in orientation of material elastic axes and crack inclination angle are investigated in the first and second examples, respectively. Both problems are analyzed using both the NURBS and T-spline based XIGA.

In order to increase the integration accuracy, the 'sub-triangles' technique with 13 Gauss points is adopted for integration over elements cut by the crack, while the 'almost polar' technique with 7×7 Gauss points is utilized for elements that contain the crack tip (see [1]). Standard 4×4 Gauss quadrature points are used for integration of other elements. For determining the fracture properties, the stress intensity factors (SIFs) are obtained by means of the interaction integral method, previously developed by Kim and Paulino [2].

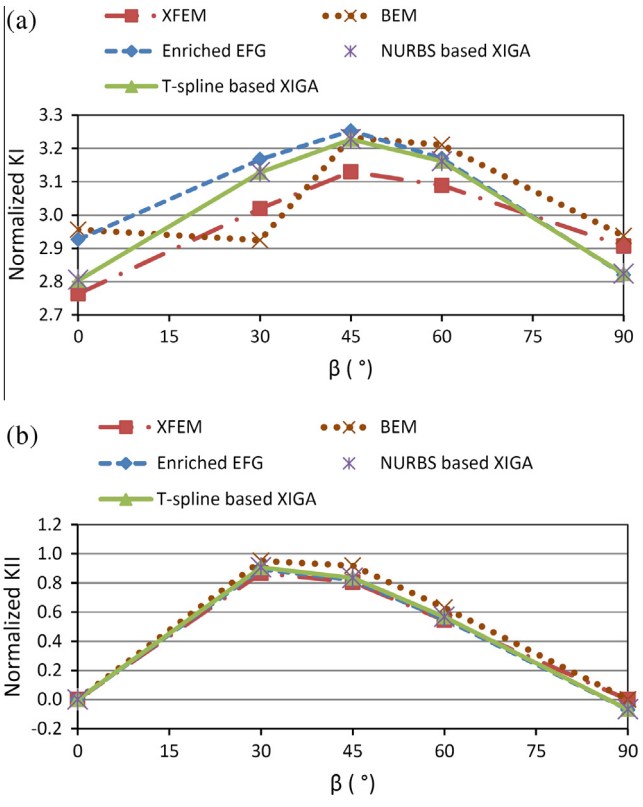

Fig. 7. The effect of various inclinations of elastic material axes on the mixed mode SIFs: (a) normalized mode I SIF ($\frac{K_I}{\sigma_o\sqrt{\pi a}}$) , (b) normalized mode II SIF ($\frac{K_{II}}{\sigma_o\sqrt{\pi a}}$).

5.1. Rectangular plate with an edge crack under tension

The proposed method is applied for analysis of a finite rectangular orthotropic plate with an edge crack subjected to uni-axial tension. The plate is considered in the plane stress state and several orientations of material elastic axes are studied. The proportions of width to height and crack length to width are equal to 0.5 (see Fig. 4). The plate is composed of a graphic-epoxy material with the following orthotropic properties:

$$E_1 = 114.8\ \text{GPa}, \quad E_2 = 11.7\ \text{GPa}, \quad G_{12} = 9.66\ \text{GPa}, \quad \nu_{12} = 0.21$$

Local refinement around the crack tip is of interest. 1296 control points and 1089 elements are used for modeling the problem in a global refined form using NURBS, as illustrated in Fig. 5. By applying the T-spline basis functions, 960 control points and 825 elements are utilized for discretization of the locally refined model (see Fig. 6). Note that the elements used for integration are projection of the union of knot lines and continuity reduction lines in the physical space, while the physical mesh is defined by projection of knot lines in the physical space (see [53] for more details). The

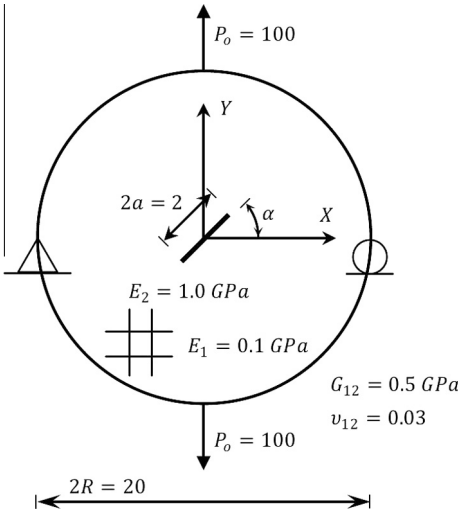

Fig. 8. Geometry and boundary conditions of the orthotropic disk with an inclined central crack.

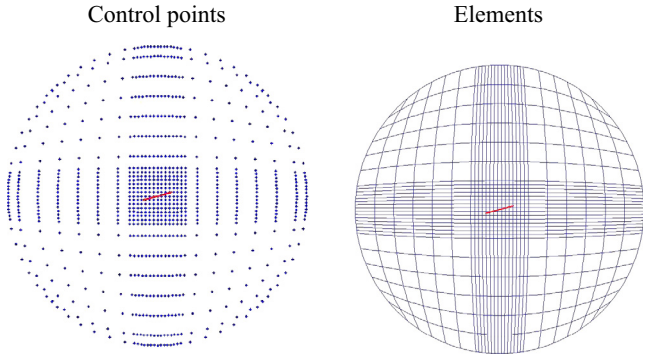

Fig. 9. Discretization of the globally refined model of cracked orthotropic disk.

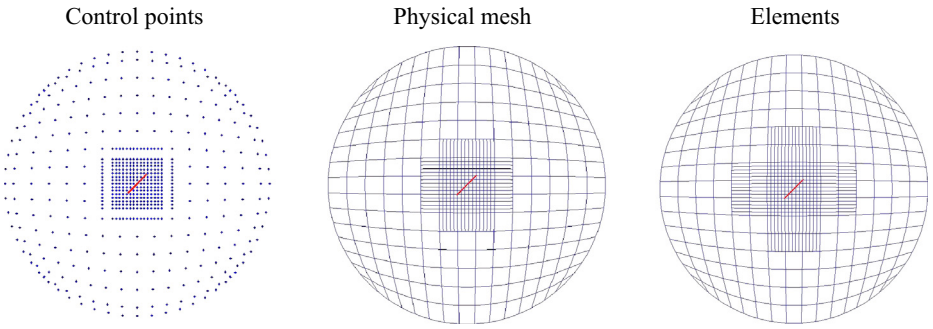

Fig. 10. Discretization of the locally refined model of cracked orthotropic disk.

Table 1
Stress intensity factors for an inclined central crack in an orthotropic disk subjected to point loads ($\alpha = 30^\circ$).

Method	DOFs	Elements	Cells	K_I	K_{II}
MCC [34]	5424	999	–	16.73	11.33
M-integral [34]	5424	999	–	16.75	11.38
XFEM [37]	1960	920	–	17.08	11.65
Enriched EFG [38]	1507	–	641	16.98	11.95
NURBS based XIGA	1868	729	–	16.98	11.53
T-spline based XIGA	1292	537	–	17.01	11.55

minimum and maximum sizes of elements are $[w \times h]/27^2$ and $[w \times h]/27$ around the crack tip and far from it, respectively. Cubic basis functions are adopted for the analysis.

For comparing the obtained results with those available in the literature, the Stress Intensity Factor (SIF) is calculated by the technique developed by Kim and Paulino [2]. Effects of changing the material elastic angle on mixed mode SIFs in the plate are probed. Comparison of the results of the proposed method and the results of the enriched element free Galerkin (EFG) [38], the extended finite element method (XFEM) [37] and the boundary element method (BEM) [33], is shown in Fig. 7.

It is observed that the results are in good agreement with those obtained by other methods. The results show that the trend of mode I SIF changes around $\beta = 45^\circ$. It has an increasing trend in the span of $\beta = 0^\circ$ to $\beta = 45^\circ$ and then decreases in the span of $\beta = 45^\circ$ to $\beta = 90^\circ$ and reaches a value around its initial value, i.e. when $\beta = 0^\circ$. The turning point for the mode II SIF is about $\beta = 30^\circ$. It should be emphasized that the same level of accuracy is obtained with T-spline XIGA by much lower number of DOFS, control points and elements.

5.2. Disk with an inclined central crack subjected to point loads

Consider an orthotropic disk with an inclined central crack subjected to double point loads, as depicted in Fig. 8. The material orthotropy axes and corresponding material properties are defined in Fig. 8.

For discretization purpose, the area around the crack is refined and both global (Fig. 9) and local (Fig. 10) refinements using quadratic degree NURBS and T-spline basis functions are employed.

Table 1 compares the stress intensity factors reported by Kim and Paulino [34], Asadpoure and Mohammadi [37] and Ghorashi et al. [38] with those obtained using the present approach for the case of $\alpha = 30^\circ$.

XIGA is also used for analysis of different inclination angles of the crack. The computed values of mixed mode SIFs alongside those reported by Asadpoure and Mohammadi [37] and Ghorashi et al. [38] are illustrated in Fig. 11. The results of XIGA are in good agreement with the others. Note that similar to XFEM and EFG methods, XIGA is capable of analyzing several crack inclination problems on only one discretization.

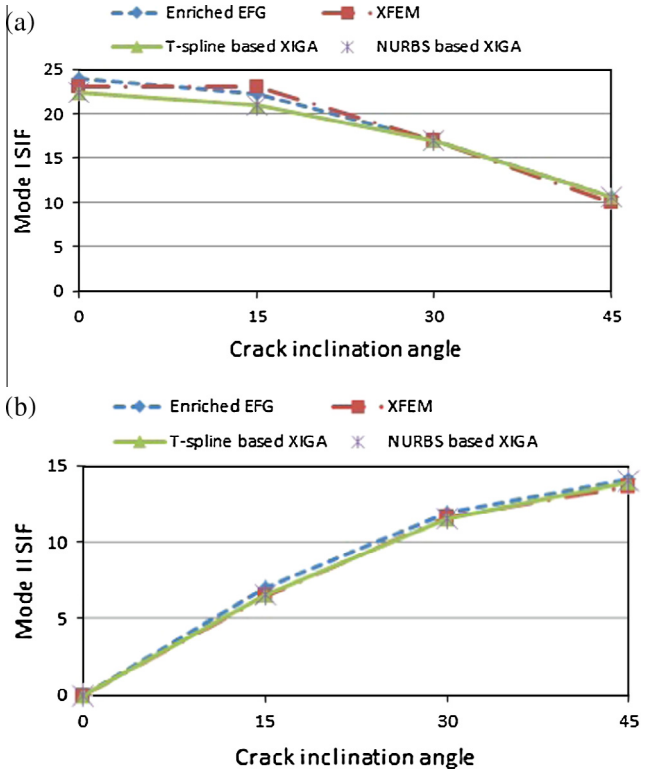

Fig. 11. SIF values corresponding to different central crack angles in the orthotropic disk: (a) mode I SIFs; (b) mode II SIFs.

6. Conclusion

In this contribution, the newly developed XIGA has been extended to analysis of cracked orthotropic plates. The recently proposed crack-tip orthotropic enrichment functions have been employed in the XIGA method to increase the approximation accuracy near the crack-tip. Furthermore, by adopting the T-spline basis functions, the proposed approach allows for efficient local refinements.

The proposed approach have been utilized to analyze some numerical examples. Results of mixed-mode stress intensity factors (SIFs) have been compared with the reference results and proved the accuracy and efficiency of the method.

By adopting an appropriate error estimator in the developed scheme, which is in progress by the authors, efficient adaptive procedures can now be followed.

Acknowledgement

This research is mainly supported by the German Research Institute (DFG) via Research Training Group "Evaluation of Coupled Numerical Partial Models in Structural Engineering (GRK 1462)", which is gratefully acknowledged by the first author.

The second and fourth authors would like to acknowledge the financial support of the Framework Program 7 Initial Training Network Funding under Grant No. 289361 "Integrating Numerical Simulation and Geometric Design Technology".

References

[1] Ghorashi SSh, Valizadeh N, Mohammadi S. Extended isogeometric analysis (XIGA) for simulation of stationary and propagating cracks. Int J Numer Methods Eng 2012;89:1069–101.
[2] Kim JH, Paulino GH. The interaction integral for fracture of orthotropic functionally graded materials: evaluation of stress intensity factors. Int J Solids Struct 2003;40:3967–4001.
[3] Sih GC, Paris PC, Irwin GR. On cracks in rectilinearly anisotropic bodies. Int J Fract Mech 1965;1:189–203.
[4] Muskelishvili NI. Some basic problems on the mathematical theory of elasticity. Groningen: Noordhoof; 1952.
[5] Lekhnitskii SG. Theory of an anisotropic elastic body. San Francisco: Holden-Day; 1963.
[6] Bowie OL, Freese CE. Central crack in plane orthotropic rectangular sheet. Int J Fract Mech 1972;8(1):49–58.
[7] Kuo MC, Bogy DB. Plane solutions for the displacement and traction-displacement problem for anisotropic elastic wedges. J Appl Mech 1974;41:197–203.
[8] Viola A, Piva A, Radi E. Crack propagation in an orthotropic medium under general loading. Eng Fract Mech 1989;34(5):1155–74.
[9] Lim WK, Choi SY, Sankar BV. Biaxial load effects on crack extension in anisotropic solids. Eng Fract Mech 2001;68:403–16.
[10] Nobile L, Carloni C. Fracture analysis for orthotropic cracked plates. Compos Struct 2005;68(3):285–93.
[11] Belytschko T, Lu YY, Gu L. Element-free Galerkin methods. Int J Numer Methods Eng 1994;37:229–56.
[12] Liu WK, Jun S, Zhang YF. Reproducing kernel particle methods. Int J Numer Methods Eng 1995;20:1081–106.
[13] Liszka TJ, Duarte CA, Tworzydlo WW. Hp-meshless cloud method. Comput Methods Appl Mech Eng 1996;139:263–88.
[14] Atluri SN, Zhu T. A new meshless local Petrov–Galerkin (MLPG) approach in computational mechanics. Comput Mech 1998;22:117–27.
[15] Gingold RA, Monaghan JJ. Smoothed particle hydrodynamics: theory and application to non-spherical stars. Monthly Notices Roy Astronom Soc 1977;181:375–89.
[16] Belytschko T, Krongauz Y, Organ D, Fleming M, Krysl P. Meshless methods: an overview and recent developments. Comput Methods Appl Mech Eng 1996;139(1–4):3–47.
[17] Rabczuk T, Belytschko T. Cracking particles: a simplified meshfree method for arbitrary evolving cracks. Int J Numer Methods Eng 2004;61(13):2316–43.
[18] Nguyen VP, Rabczuk T, Bordas S, Duflot M. Meshless methods: a review and computer implementation aspects. Math Comput Simul 2008;79(3):763–813.
[19] Cai Y, Zhuang X, Zhu H. A generalized and efficient method for finite cover generation in the numerical manifold method. Int J Comput Methods 2013;10(5). Art. No. 1350028.
[20] Zhuang X, Augarde CE, Mathisen KM. Fracture modeling using meshless methods and level sets in 3D: framework and modeling. Int J Numer Methods Eng 2012;92(11):969–98.
[21] Zhu H, Zhuang X, Cai Y, Ma G. High rock slope stability analysis using the enriched meshless shepard and least squares method. Int J Comput Methods 2011;8(2):209–28.
[22] Belytschko T, Black T. Elastic crack growth in finite elements with minimal remeshing. Int J Numer Methods Eng 1999;45:601–20.
[23] Moës N, Dolbow J, Belytschko T. A finite element method for crack growth without remeshing. Int J Numer Methods Eng 1999;46:131–50.
[24] Mohammadi S. Extended finite element method for fracture analysis of structures. United Kingdom: Wiley/Blackwell; 2008.
[25] Rabczuk T, Zi G, Bordas S, Nguyen-Xuan H. A simple and robust three-dimensional cracking-particle method without enrichment. Comput Methods Appl Mech Eng 2010;199(37–40):2437–55.
[26] Rabczuk T, Belytschko T. A three dimensional large deformation meshfree method for arbitrary evolving cracks. Comput Methods Appl Mech Eng 2007;196(29–30):2777–99.
[27] Rabczuk T, Areias PMA, Belytschko T. A meshfree thin shell method for nonlinear dynamic fracture. Int J Numer Methods Eng 2007;72(5):524–48.
[28] Rabczuk T, Zi G. A meshfree method based on the local partition of unity for cohesive cracks. Comput Mech 2007;39(6):743–60.
[29] Rabczuk T, Bordas S, Zi G. On three-dimensional modelling of crack growth using partition of unity methods. Comput Struct 2010;88(23–24):1391–411.
[30] Fries T-P, Belytschko T. The extended/generalized finite element method: an overview of the method and its applications. Int J Numer Methods Eng 2010;84(3):253–304.
[31] Mohammadi S. XFEM fracture analysis of composites. Chichester, United Kingdom: John Wiley & Sons, Ltd; 2012.
[32] Atluri SN, Kobayashi AS, Nakagaki M. Finite element program for fracture mechanics analysis of composite material, fracture mechanics of composites. ASTM STP, Am Soc Test Mater 1975;593:86–98.
[33] Aliabadi MH, Sollero P. Crack growth analysis in homogeneous orthotropic laminates. Compos Sci Technol 1998;58:1697–703.
[34] Kim JH, Paulino GH. Mixed-mode fracture of orthotropic functionally graded materials using finite elements and the modified crack closure method. Eng Fract Mech 2002;69:1557–86.
[35] Asadpoure A, Mohammadi S, Vafai A. Modeling crack in orthotropic media using a coupled finite element and partition of unity methods. Finite Elem Anal Des 2006;42(13):1165–75.
[36] Asadpoure A, Mohammadi S, Vafai A. Crack analysis in orthotropic media using the extended finite element method. Thin-Wall Struct 2006;44(9):1031–8.
[37] Asadpoure A, Mohammadi S. Developing new enrichment functions for crack simulation in orthotropic media by the extended finite element method. Int J Numer Methods Eng 2007;69(10):2150–72.
[38] Ghorashi SSh, Mohammadi S, Sabbagh-Yazdi SR. Orthotropic enriched element free Galerkin method for fracture analysis of composites. Eng Fract Mech 2011;78:1906–27.
[39] Motamedi D, Mohammadi S. Dynamic analysis of fixed cracks in composites by the extended finite element method. Eng Fract Mech 2010;77:3373–93.
[40] Motamedi D, Mohammadi S. Dynamic crack propagation analysis of orthotropic media by the extended finite element method. Int J Fract 2010;161:21–39.
[41] Esna Ashari S, Mohammadi S. Delamination analysis of composites by new orthotropic bimaterial extended finite element method. Int J Numer Methods Eng 2011;86(13):1507–43.
[42] De Luycker E, Benson DJ, Belytschko T, Bazilevs Y, Hsu MC. X-FEM in isogeometric analysis for linear fracture mechanics. Int J Numer Methods Eng 2011;87:541–65.
[43] Hughes TJR, Cottrell JA, Bazilevs Y. Isogeometric analysis: CAD, finite elements, NURBS, exact geometry and mesh refinement. Comput Methods Appl Mech Eng 2005;194:4135–95.
[44] Cottrell JA, Hughes TJR, Bazilevs Y. Isogeometric analysis: towards integration of CAD and FEA. Chichester: Wiley; 2009.
[45] Verhoosel CV, Scott MA, Hughes TJR, de Borst R. An isogeometric analysis approach to gradient damage models. Int J Numer Methods Eng 2011;86(1):115–34.
[46] Verhoosel CV, Scott MA, de Borst R, Hughes TJR. An isogeometric approach to cohesive zone modeling. Int J Numer Methods Eng 2011;87(1–5):336–60.
[47] Ghorashi SSh, Valizadeh N, Mohammadi S, Rabczuk T. Extended isogeometric analysis of plates with curved cracks. In: Topping BHV, editor. Proceedings of the eighth international conference on engineering computational technology. Stirlingshire, UK: Civil-Comp Press; 2012. Paper 47, http://dx.doi.org/10.4203/ccp.100.47.
[48] Lahmer T, Ghorashi SSh. Extended isogeometric analysis based crack identification applying multilevel regularizing methods. In: 19th International conference on the application of computer science and mathematics in architecture and civil engineering, Weimar, Germany; 2012.
[49] Jia Y, Anitescu C, Ghorashi SSh, Rabczuk T. Extended isogeometric analysis for material interface problems. IMA J Appl Math 2014. http://dx.doi.org/10.1093/imamat/hxu004.
[50] Cottrell JA, Hughes TJR, Reali A. Studies of refinement and continuity in isogeometric structural analysis. Comput Methods Appl Mech Eng 2007;196:4160–83.
[51] Jia Y, Zhang Y, Xu G, Zhuang X, Rabczuk T. Reproducing kernel triangular B-spline-based FEM for solving PDEs. Comput Methods Appl Mech Eng 2013;267:342–58.
[52] Sederberg TW, Zheng J, Bakenov A, Nasri A. T-splines and T-NURCCSs. ACM Trans Graph 2003;22(3):477–84.
[53] Bazilevs Y, Calo VM, Cottrell JA, Evans JA, Hughes TJR, Lipton S, et al. Isogeometric analysis using T-splines. Comput Methods Appl Mech Eng 2010;199(5–8):229–63.
[54] Dörfel MR, Jüttler B, Simeon B. Adaptive isogeometric analysis by local h-refinement with T-splines. Comput Methods Appl Mech Eng 2010;199(5–8):264–75.
[55] Li X, Zheng J, Sederberg TW, Hughes TJR, Scott MA. On linear independence of T-spline blending functions. Comput Aid Geometr Des 2012;29:63–76.
[56] Scott MA, Li X, Sederberg TW, Hughes TJR. Local refinement of analysis-suitable T-splines. Comput Methods Appl Mech Eng 2012;213–216:206–22.
[57] Deng J, Chen F, Li X, Changqi H, Tong W, Yang Z, et al. Polynomial splines over hierarchical T-meshes. Graph Models 2008;70(4):76–86.
[58] Nguyen-Thanh N, Muthu J, Zhuang X, Rabczuk T. An adaptive three-dimensional RHT-spline formulation in linear elasto-statics and elasto-dynamics. Comput Mech 2014;53(2):369–85.
[59] Nguyen-Thanh N, Kiendl J, Nguyen-Xuan H, Wüchner R, Bletzinger KU, Bazilevs Y, et al. Rotation free isogeometric thin shell analysis using PHT-splines. Comput Methods Appl Mech Eng 2011;200(47–48):3410–24.
[60] Nguyen-Thanh N, Nguyen-Xuan H, Bordas SPA, Rabczuk T. Isogeometric analysis using polynomial splines over hierarchical T-meshes for two-

dimensional elastic solids. Comput Methods Appl Mech Eng 2011;200(21–22):1892–908.

[61] Ghorashi SSh, Valizadeh N, Mohammadi S. Orthotropic enriched XIGA for fracture analysis of composites. In: Topping BHV, editor. Proceedings of the eighth international conference on engineering computational technology. Stirlingshire, UK: Civil-Comp Press; 2012. Paper 46, http://dx.doi.org/10.4203/ccp.100.46.

[62] Piegl L, Tiller W. The NURBS book (monographs in visual communication). 2nd ed. New York: Springer-Verlag; 1997.

[63] Ghorashi SSh, Rabczuk T, Ródenas JJ, Lahmer T. T-spline based XIGA for adaptive modeling of cracked bodies. In: 19th International conference on the application of computer science and mathematics in architecture and civil engineering, Weimar, Germany; 2012.